

## Ultra-wideband Antenna based on Composite Right and Left Handed Transmission Lines

Jiixin Wang, Li He

Chongqing University of Posts and Telecommunications, Chongqing, 400065, China.

### Abstract

Based on the theory of composite right and left handed transmission lines, an ultra-wideband antenna with a size of  $20 \times 18 \times 1.6$  mm<sup>3</sup> is designed by using asymmetric coplanar waveguide feed. The antenna is composed of a monopole antenna, an interdigital capacitor on the end wall and a bending inductance on the side wall. The simulation results of HFSS show that the designed antenna covers 2.3~11.6 GHz bandwidth with a relative bandwidth of 133.8%. In addition, the antenna has negative dielectric constant characteristics. The antenna has the advantages of small size, bandwidth and simple structure, and has wide application value.

### Keywords

CRLH-TL, UWB, Antenna.

### 1. Introduction

Metamaterials have attracted worldwide attention because of their special properties that conventional materials do not possess[1]. Up to now, the main metamaterials are composite right and left handed transmission lines, left handed materials and so on[2]. Composite right and left handed transmission lines have many supernormal characteristics, such as zero-order resonance, inverse Doppler effect, negative refractive index, etc. [3-4]. Among them, the zero-order resonance has an important characteristic that its resonance frequency is independent of size [5]. Therefore, this characteristic can be used to realize the miniaturization of antenna[6].

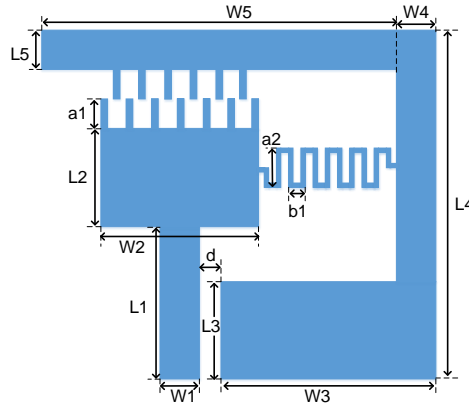
Since the composite right handed transmission line was proposed, there has been an endless stream of research teams at home and abroad. In 2002, Caloz et al. proposed that the hybrid right handed transmission line be used to realize the anisotropic characteristic [7]. In 2009, literature [8] fused the resonant frequency of monopole oscillator and the resonant frequency of metamaterial within a bandwidth by loading the composite right handed transmission line structure, thus realizing the broadband characteristic. Then, the research of broadband metamaterial antenna emerges in endlessly, such as short-ended[9], strip antenna[10], metamaterial array[11] is widely used. Multifrequency fusion to broaden bandwidth is the development trend of metamaterials nowadays.

In this paper, a epsilon negative transmission line (ENG-TL) antenna based on composite right and left handed transmission lines is proposed. The antenna is miniaturized by using zero-order resonance characteristics. The ultra-wideband function is realized by feeding ACPW.

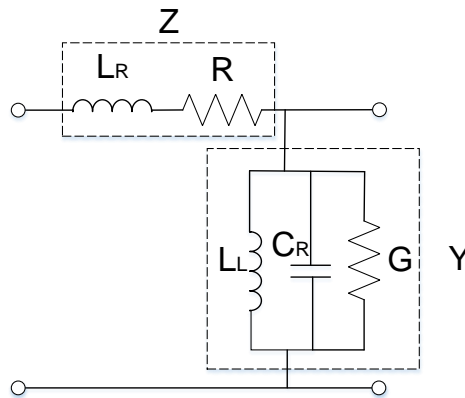
### 2. Structure Design of Antenna

Based on CRLH theory, an ultra-wideband antenna fed by asymmetric coplanar waveguide (ACPW) is designed, as shown in Fig. 1 (a). The antenna is fabricated on FR4 ( $\epsilon_r = 4.4$ ,  $\tan \sigma = 0.02$ ) dielectric plate with a thickness of 1.6 mm and a radiation structure consisting of copper with a thickness of 0.017 mm. With asymmetric coplanar waveguide feeding, the antenna size is greatly reduced by half of the area saved compared with the traditional coplanar waveguide feeding because it has only one side. The bending structure provides a left-handed inductance, which can be controlled by adjusting the length and width of the bending and the size of the inductance. Because the antenna fabricated by CRLH theory has negative dielectric constant and negative permeability, the antenna designed by ENG theory only has negative dielectric constant, and CRLH has only one more series capacitance than ENG in the equivalent circuit. Therefore, they are similar in the analysis of the equivalent circuit

of antenna. The interdigital structure strengthens the coupling between the radiation patch and the ground, and forms the right-handed capacitance, coupled with the right-handed inductance generated by the radiation patch itself. Thus forming the epsilon negative transmission line (ENG-TL) structure, whose equivalent circuit is shown in Figure 1 (b). The series impedance and parallel admittance in the figure are following.



(a) Element ENG-TL Antenna Structural Diagram(W1=2 mm, L1=8 mm, W2=8 mm, L2=5 mm, W3=11 mm, L3=5 mm, W4=2 mm, L4=18 mm, W5=18 mm, L5=2 mm, a1=1.6 mm, a2=2 mm, b1=0.84 mm)



(b) Antenna equivalent circuit diagram

Fig. 1. Schematic diagram and equivalent circuit diagram of unit antenna

$$Z = j\omega L_R + R \tag{1}$$

$$Y = j\omega C_R + 1/j\omega L_L + G \tag{2}$$

R and G are the impedance and admittance of the lossy circuit respectively. Under ideal lossless condition, the imaginary part of the shunt admittance is zero, so the zero-order resonance frequency is as follow.

$$\omega = 1/\sqrt{C_R L_L} \tag{3}$$

According to Bloch-Floquet theory [12], the dispersion characteristics of composite right and left handed transmission lines are as follows.

$$\beta d = \cos^{-1} \left( \frac{1 - S_{11} S_{22} + S_{21}^2}{2S_{21}} \right) \tag{4}$$

Where d is the length of the unit period. According to this formula, the dispersion characteristic curve of periodic ENG-TL antenna is shown in Fig. 2 (a). The dispersion diagram is divided in left-handed and right-handed regions. The dielectric constant in 0.5 GHz-4 GHz band is negative, and then it is left handed transmission line; 3.5 GHz-4 GHz is the transition band from left handed transmission line to right handed transmission line, in which beta is a pure imaginary number; and 4 GHz-8.5 GHz

is right handed transmission line, and the real part of the corresponding dielectric constant is positive. The left-handed region represents the frequency range with negative slope of the curve, as well as the anti-parallel phase and group velocity. On the other hand, the slope of the right-hand region curve is positive, and it also represents the parallel phase and velocity.

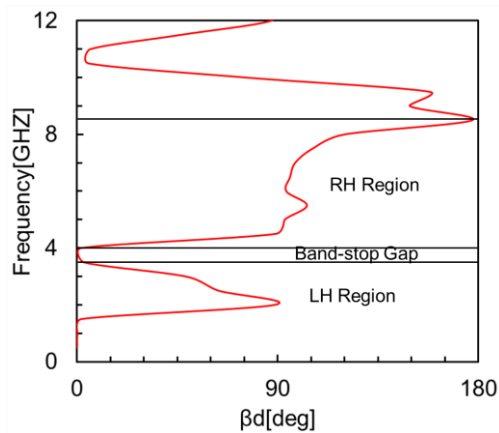
In addition, the permittivity and permeability of the antenna can be obtained by the following formula.

$$n = \frac{1}{kd} \cos^{-1} \left[ \frac{1}{2S_{21}} (1 - S_{11}^2 + S_{21}^2) \right] \tag{5}$$

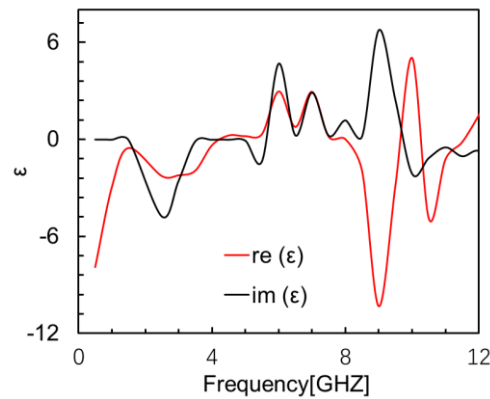
$$z = \sqrt{\frac{(1 + S_{11})^2 - S_{21}^2}{(1 - S_{11})^2 - S_{21}^2}} \tag{6}$$

$$\epsilon = n / z \tag{7}$$

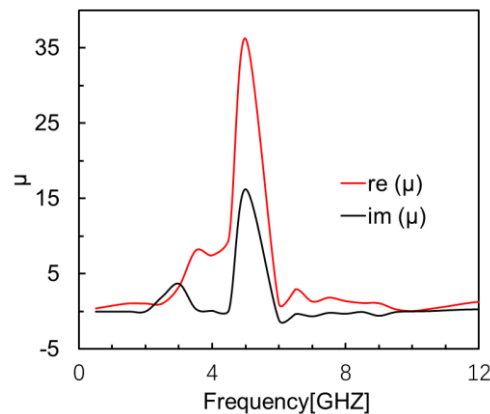
$$\mu = nz \tag{8}$$



(a) Dispersion characteristic curve of ENG-TL antenna



(b) Equivalent permittivity of ENG-TL antenna



(c) Equivalent permeability of ENG-TL antenna

Fig. 2. Key parameters of ENG-TL antenna

Where  $n$  is the refractive index and  $z$  is the wave impedance. Because the dielectric constant of ENG-TL structure is less than zero and the permeability is greater than zero, as shown in Figure 2 (c), although the permeability fluctuates, it remains positive. The three curves show that the antenna has ENG-TL function.

### 3. Antenna simulation results analysis

The structure is simulated by HFSS software, and the return loss curve of the antenna is obtained as shown in Figure 3. There are four resonant modes in the antenna, which are 3.95 GHz, 6.68 GHz, 8.19 GHz and 10.9 GHz. According to the dispersion curve of the antenna, 3.95 GHz is a zero-order resonant mode, and the antenna bandwidth is 2.3-11.6 GHz (133.8%). At the same time, CST electromagnetic simulation software is used to verify. Both softwares resonate at 6.68 GHz, 8.19 GHz and 10.9 GHz, but the 3.95 GHz resonant point moves to 1.58 GHz, which is due to the algorithm differences between the two softwares.

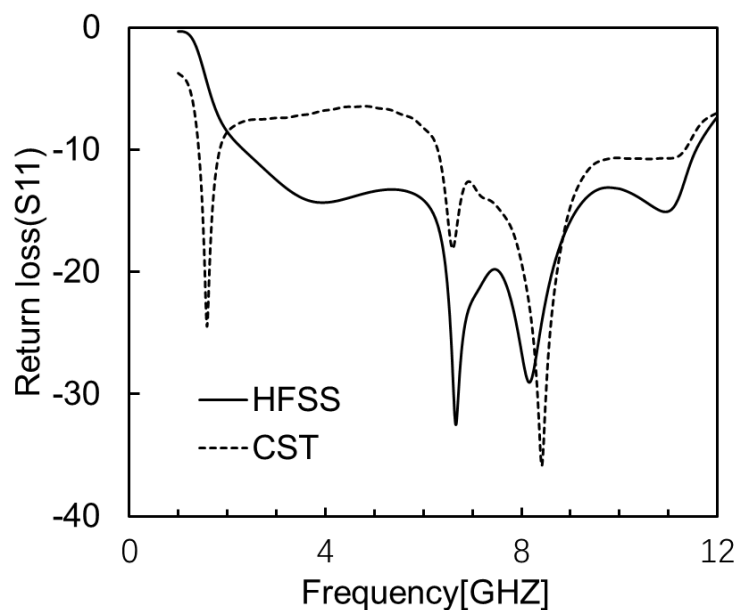


Fig. 3.ENG-TL Antenna Return Loss Curve

In order to analyze the resonant characteristics of four resonant modes in detail, the current distribution of four resonant points is shown in Fig. 4. The first resonant mode is generated by the left-handed inductance between the bent line and the ground; the second resonant mode is still coupled by the bent line and the ground, but an additional right-handed capacitor between the radiation patch and the ground is added; the third resonant mode current mainly concentrates on the bent line, compared with the first two resonant modes, the current on the bent line of this mode is obviously increased and the current on both sides is larger than that on the first two resonant modes. Intermediate current; the current on the bend line of the fourth resonant mode is concentrated in the middle. It can be seen from the figure that the resonance is mainly caused by the coupling between the bending line and the ground and the radiation patch and the ground.

Because the resonance is mainly caused by the coupling between the bending line and the ground and the radiation patch and the ground, the length of the bending line is scanned by parameters. As shown in Fig. 5 (a), the longer the length of the bending line, the larger the left-handed inductance produced by the bending line. According to  $f = 1/2\pi\sqrt{C_R L_L}$ , the larger the inductance, the smaller the resonance point. The redshift of S parameter will occur. When the distance between the patch and the ground is scanned by parameters, the coupling distance increases, the echo loss decreases and the depth increases, as shown in Fig. 5 (b).

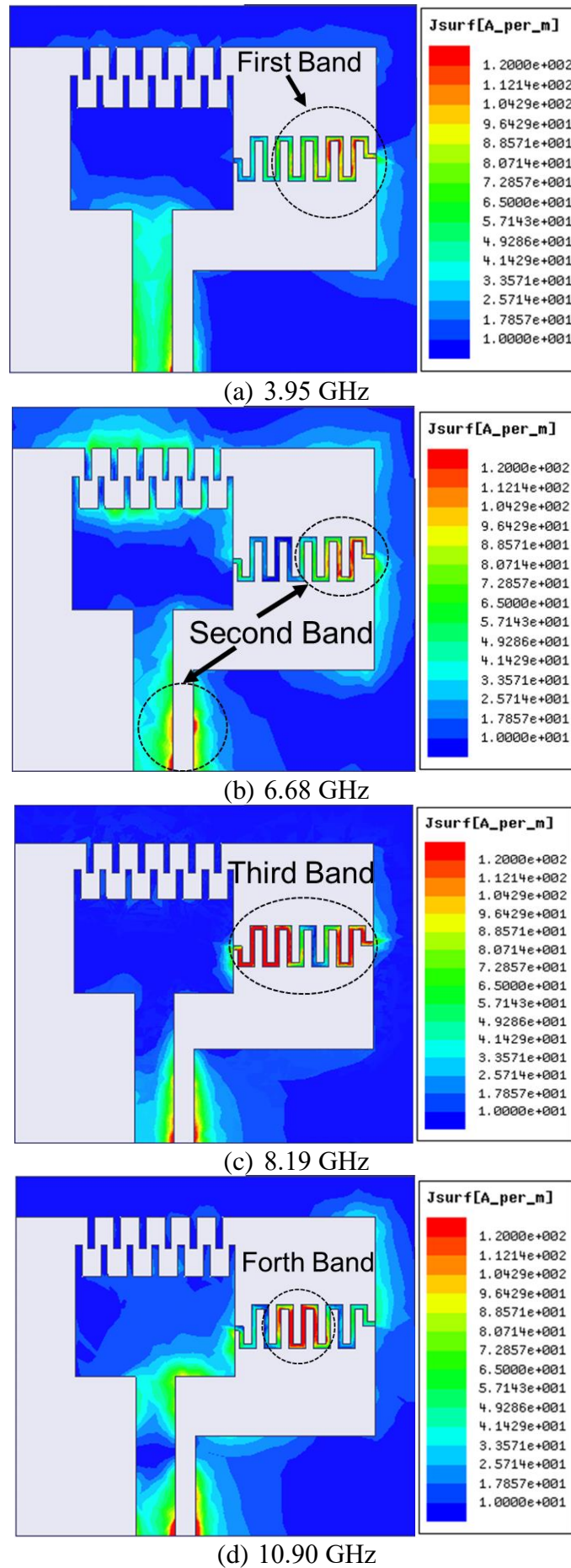
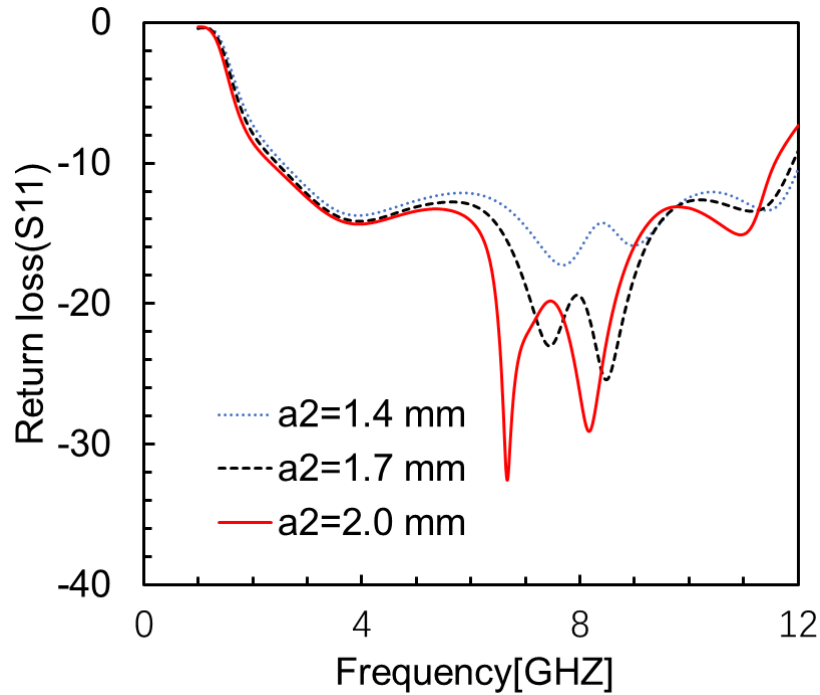
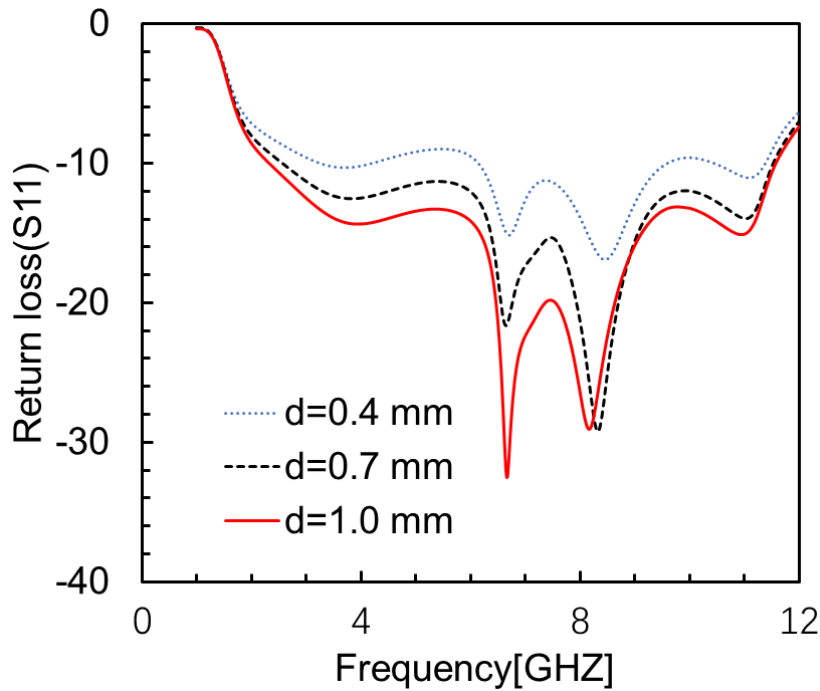


Fig. 4. Current distribution at resonant point of ENG-TL antenna



(a) Scanning of bending inductance length parameters



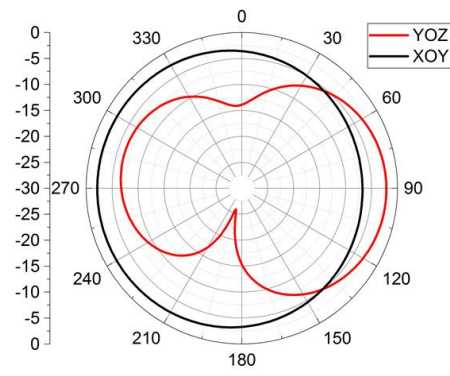
(b) Patch-to-ground coupling distance parameter scanning

Fig. 5. Parameter optimization of ENG-TL antenna

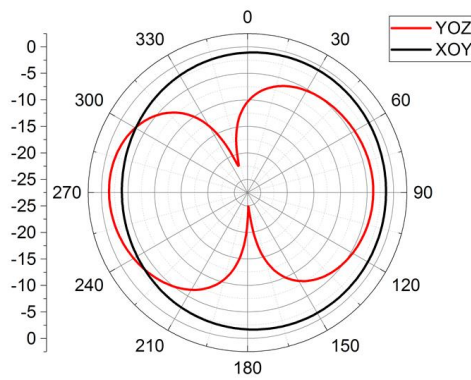
#### 4. Simulation and Analysis

The antenna pattern is shown in Figure 6. The gains of antenna at 3.95 GHz, 6.68 GHz, 8.19 GHz and 10.90 GHz are - 2.13 dBi, - 0.78 dBi, 1.42 dBi and 3.44 dBi, respectively, and they have great overall radiation on E and H planes.

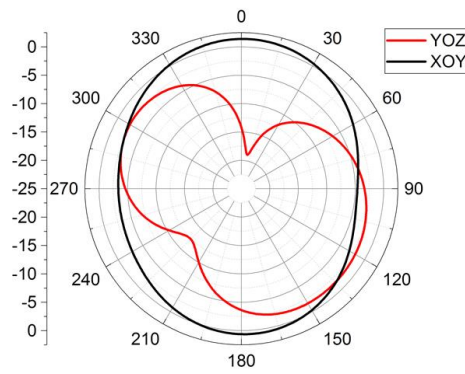
Table 1 is a comparison table of key parameters of UWB, miniature cultural antenna and reference [8-10]. It can be seen from the table that the antenna height is basically the same, and they are all designed based on composite left and right hands. However, the antenna in this paper has certain advantages in size and bandwidth.



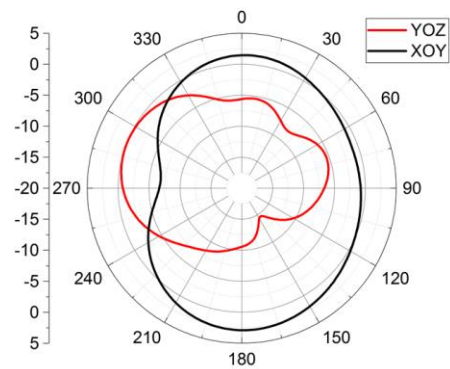
(a) 3.95 GHz



(b) 6.68 GHz



(c) 8.19 GHz



(d) 10.90 GHz

Fig. 6. Antenna resonance pattern



Table 1 Comparison table of key antenna parameters

Paper	Substrate ( $\epsilon_r$ )	Size ( $mm \times mm \times mm$ )	resonant frequency (GHz)	maximum gain(dBi)	Impedance bandwidth (GHz)
This work	FR4(4.4)	20×18×1.6	3.95	-2.13	2.3~11.6(133.8%)
			6.68	-0.78	
			8.19	1.42	
			10.90	3.44	
[13]	FR4(4.4)	42×32×1.6	0.56	—	0.56~0.58(3.5%)
			2.67	3.81	2.35~2.91(21.3%)
			3.15	3.75	2.91~3.49(18.1%)
[14]	Rogers RT/duroid 5880(2.2)	45×25×1.56	2.49	-2.00	2.37~2.64(10.8%)
			3.53	0.14	3.39~3.58(5.4%)
			5.54	3.20	4.86~6.98(38.3%)
[15]	FR4(4.4)	30×30×1.6	1.16	1.59	1.12~1.22(8.5%)
			2.32	2.10	2.22~2.46(10.3%)
			3.58	4.97	2.94~4.22(35.8%)

## 5. Conclusion

In this paper, an ENG-TL antenna is designed, which covers 2.3-11.6 GHz band and has a relative bandwidth of 133.8%. The ultra-wideband of the antenna is realized. Through the analysis of the current distribution of the antenna, the key parameters affecting the resonance point are found, which can provide reference value for practical application.

## References

- [1] Jafarholi, Ali, A. Jafarholi, and J. H. Choi. Mutual Coupling Reduction in an Array of Patch Antennas Using CLL Metamaterial Superstrate for MIMO Applications, IEEE Transactions on Antennas and Propagation (2018):1-1.
- [2] Rajkumar, Rengasamy, and U. K. Kommuri. A Triangular Complementary Split Ring Resonator Based Compact Metamaterial Antenna for Multiband Operation, Wireless Personal Communications (2018).
- [3] Cao, W. Q., et al. Novel phase-shifting characteristic of CRLH TL and its application in the design of dual-band dual-mode dual-polarization antenna, Progress In Electromagnetics Research. 131, (2012) 131.5(2012):375-390.
- [4] H. Mirzaei; G.V. Eleftheriades; A compact frequency-reconfigurable metamaterial-inspired antenna, IEEE Antennas and Wireless Propagation Letters, 2011, vol. 10, p. 1154-1157.
- [5] Ibrahim, Ahmed A., M. A. Abdalla, and H. Zhirun. Compact ACS-fed CRLH MIMO antenna for wireless applications, IET Microwaves, Antennas & Propagation 12.6(2018):1021-1025.
- [6] Mishra N, Chaudhary R K. A Miniaturized ZOR antenna with enhanced bandwidth for WiMAX applications, Microwave and Optical Technology Letters, 2016, 58(1):71-75.
- [7] Caloz, C., A. Sanada, and T. Itoh. A novel composite right-/left-handed coupled-line directional coupler with arbitrary coupling level and broad bandwidth, IEEE Transactions on Microwave Theory and Techniques 52.3(2004):980-992.
- [8] Antoniadou, Marco A., and G. V. Eleftheriades. A Broadband Dual-Mode Monopole Antenna Using NRI-TL Metamaterial Loading, IEEE Antennas and Wireless Propagation Letters 8.4(2009): 258-261.
- [9] Mishra, Naveen, and R. K. Chaudhary. A COMPACT WIDEBAND SHORT-ENDED METAMATERIAL ANTENNA FOR WIRELESS APPLICATIONS, Progress In Electromagnetics Research Letters 66(2017):93-98.



- 
- [10] ShengJun Wei; QuanYuan Feng. An asymmetric coplanar waveguide (ACPW) resonant antenna based on the composite right/left-handed transmission line, *Science China Information Sciences*, 2013, vol. 56, no. 12, p. 1–9.
- [11] Mishra N, Chaudhary R K. A COMPACT CPW FED CRR LOADED FOUR ELEMENT METAMATERIAL ARRAY ANTENNA FOR WIRELESS APPLICATION, *Progress In Electromagnetics Research*, 2017, 159:15-26.
- [12] Lai, Anthony, K. M. K. H. Leong , and T. Itoh. Infinite Wavelength Resonant Antennas With Monopolar Radiation Pattern Based on Periodic Structures, *IEEE Transactions on Antennas and Propagation* 55.3(2007):868-876.
- [13] Hasan, Md. Mehedi, M. R. I. Faruque , and M. T. Islam. Dual Band Metamaterial Antenna For LTE/ Bluetooth/ WiMAX System, *cientific Reports* 8.1(2018):1240.
- [14] Nandi, Sourav, and A. Mohan . CRLH Unit Cell Loaded Tri-Band Compact MIMO Antenna for WLAN/WiMAX Applications, *IEEE Antennas and Wireless Propagation Letters* (2017):1-1.
- [15] Kumar, Rajkishor, R. Singh , and R. K. Chaudhary. Miniaturised triple-band antenna loaded with complementary concentric closed ring resonators with asymmetric coplanar waveguide-fed based on epsilon negative transmission line, *IET Microwaves Antennas & Propagation* 12.13(2018): 2073-2079.